Charge Exchange Cross Sections of Hydrogen Ions in Gases

P. M. STIER* AND C. F. BARNETT
Oak Ridge National Laboratory, Oak Ridge, Tennessee
(Received March 28, 1956; revised version received May 28, 1956)

Measurements are reported of the cross section for electron capture (σ_{10}), electron loss (σ_{01}), and electron detachment (σ_{-10}) for hydrogen atoms and ions traversing several gases. (σ_{if} represents the cross section for charge transfer from initial state i to final state f.) The kinetic energy of the particle was from 3 kev to 200 kev. The target gases used were H_2, He, N_2, O_2, Ne, and A. Cross sections were determined by measuring the attenuation of the hydrogen beam in a gas cell under the influence of an electrostatic or magnetic field. The fraction of the beam in each charge state after passing through a "thick target" was also determined. This latter measurement served as a test for internal consistency of the data, since the fraction is relatable to the cross section for entry to and exit from the charge state. The loss cross section, σ_{01}, increased monotonically at low energies, reaching a maximum at a velocity approximately equal to the orbital electron velocity. For the higher energies studied the capture cross section could be represented by an expression of the form, $\sigma = Ae^{-bv}$, where A and b are constants for each gas studied. The electron attachment cross section, σ_{0-1}, was of the order 10^{-17} cm^2/gas atom for the gases studied and attained a maximum between 5 and 20 kev. The inverse transition, σ_{-10}, was approximately 10^{-15} cm^2/gas atom in the energy range studied.

I. INTRODUCTION

THIS paper is the second of a series reporting experimental determinations of the charge exchange cross sections for low-energy ions passing through gases. In the previous paper,[1] henceforth referred to as (I), the ratios of the electron loss to electron capture cross sections were presented for each of the ions H^+, He^+, N^+, Ne^+, and A^+ passing through the gases hydrogen, helium, nitrogen, oxygen, neon, and argon. These were determined by observing the charge distribution in the particle beam after traversing sufficient gas for equilibrium to be established between competing electron transfer processes. The present paper reports several experiments in which the absolute cross sections were measured for electron capture and loss by a fast hydrogen atom or ion. The stopping gases were those listed above and the energy range was from 3 to 200 kev.

The excellent reviews by Massey and Burhop[2] and by Allison and Warshaw[3] evaluate the charge exchange cross-section measurements prior to their publication dates of 1952 and 1953 respectively. Several additional papers have appeared since these summaries. Whittier[4] has reported a study whose emphasis was on the behavior of fast negative ions in hydrogen gas. Stedeford and Hasted[5] have presented extensions of the work by Hasted[6] and by Keene,[7] and give results of measurements of the cross sections for the capture of an electron by a proton and the detachment of an electron from a negative hydrogen ion. Bates, Dalgarno, Griffing and their co-workers[8] have presented a series of detailed calculations of the processes involved in inelastic collisions, particularly of charge exchange. Another theoretical calculation of the cross section for electron capture by a proton in hydrogen gas has been given by Jackson and Schiff.[9] These more recent experimental and theoretical results of studies of electron capture and loss will be included in the graphs of the data reported by this paper.

In view of the rather wide discrepancies appearing in the literature of inelastic energy loss processes, a considerable number of overdeterminations were designed into the present set of experiments. It has been the hope that the additional labor would be worthwhile, in the sense that it would test for consistency and correctness of the data obtained.

II. THEORY

The differential equations representing transitions between the possible charge states can be solved[10] for the fraction of the particle beam in each state as a function of the amount of stopping material traversed. For hydrogen ions at low energies three charge states are of importance, (−1, 0, and +1). The fraction of the particle beam, ϕ_i, in charge state i after passage through sufficient gas for equilibrium between com-

* Now at National Carbon Research Laboratories, Cleveland, Ohio.

[1] Stier, Barnett, and Evans, Phys. Rev. **96**, 973 (1954).

[2] H. S. W. Massey and E. H. S. Burhop, *Electronic and Ionic Impact Phenomena* (Clarendon Press, Oxford, 1952).

[3] S. K. Allison and S. D. Warshaw, Revs. Modern Phys. **25**, 779 (1953).

[4] A. C. Whittier, Can. J. Phys. **32**, 275 (1954).

[5] J. B. H. Stedeford and J. B. Hasted, Proc. Roy. Soc. (London) **A227**, 466 (1955).

[6] J. B. Hasted, Proc. Roy. Soc. (London) **A212**, 235 (1952).

[7] J. P. Keene, Phil. Mag. **40**, 369 (1949).

[8] D. R. Bates and A. Dalgarno, Proc. Phys. Soc. (London) **A65**, 919 (1952); A. Dalgarno and H. N. Yadav, Proc. Phys. Soc. (London) **A66**, 173 (1953); D. R. Bates and G. Griffing, Proc. Phys. Soc. (London) **A66**, 961 (1953); D. R. Bates and A. Dalgarno, Proc. Phys. Soc. (London) **A66**, 972 (1953); Bransden, Dalgarno, and King, Proc. Phys. Soc. (London) **A67**, 1075 (1954).

[9] J. D. Jackson and H. Schiff, Phys. Rev. **89**, 359 (1953).

[10] Detailed solution for several cases are given in the review article by Allison and Warshaw (reference 3). In view of this, we will not develop the equations or solutions, but refer the interested reader to the review. Only equations pertinent to the present experiments are given here. Attention is called to the typographical errors in reference 3 as pointed out by J. A. Phillips and J. L. Tuck [Rev. Sci. Instr. **27**, 97 (1956)].

peting electron capture and loss reactions is

$$\phi_{-1}=\sigma_{0-1}\sigma_{10}/D_0, \quad \phi_0=\sigma_{-10}\sigma_{10}/D_0, \quad \phi_1=\sigma_{-10}\sigma_{01}/D_0, \quad (1)$$

where

$$D_0=\sigma_{-10}(\sigma_{01}+\sigma_{10})+\sigma_{0-1}\sigma_{10}.$$

Here σ_{if} denotes the cross section for transitions from initial charge state i to final state f. The assumption is made that the cross section for transfer of two electrons in a single collision is considerably smaller than that for one electron transfer, i.e., σ_{-11} and σ_{1-1} are considered negligible.[11] It follows immediately that the ratio of the number of particles in adjacent states is the ratio of cross sections for transitions between these states:

$$\phi_{-1}/\phi_0=\sigma_{0-1}/\sigma_{-10}, \quad \phi_0/\phi_1=\sigma_{10}/\sigma_{01}. \quad (2)$$

The differential equations for the change in the flux of particles n_i in state i are

$$dn_0/d\pi=-n_0(\sigma_{0-1}+\sigma_{01})+n_1\sigma_{10}+n_{-1}\sigma_{-10}, \quad (3)$$

$$dn_{-1}/d\pi=-n_{-1}\sigma_{-10}+n_0\sigma_{0-1}, \quad (4)$$

$$dn_1/d\pi=-n_1\sigma_{10}+n_0\sigma_{01}. \quad (5)$$

Here $\pi=Ll\xi P/RT$ is the atoms presented by the target gas per sq cm, where L is Avogadro's number, l is the thickness of the gas target, ξ represents the number of atoms per molecule in the gas which is at pressure P, absolute temperature T, and R is the gas constant.

If by suitable experimental means, particles which change charge are removed, the integrals of these equations become simple exponential function of the amount of gas traversed π. Thus, if a flux N_0 of fast atoms is incident on a region of gas, and ions are removed as formed, from Eq. (3) we find the flux of atoms a distance l within the gas is given by

$$n_0=N_0e^{-\pi(\sigma_{01}+\sigma_{0-1})}. \quad (6)$$

Similarly, from Eqs. (4) and (5), for incident negative and positive ion beams, we find

$$n_{-1}=N_{-1}e^{-\pi\sigma_{-10}}, \quad (7)$$

and

$$n_1=N_1e^{-\pi\sigma_{10}}. \quad (8)$$

It will be shown (Sec. IV) that for energies greater than approximately 30 kev, the formation of negative ions is improbable and may be neglected, i.e., $\sigma_{0-1}\cong 0$. The differential equation (3) becomes

$$dn_0/d\pi=-n_0\sigma_{01}+n_1\sigma_{10}.$$

Without ion removal, the fraction of the beam which is neutral after passage through a length l of gas is

$$n_0/N_0=(1-\phi_0)e^{-\pi(\sigma_{01}+\sigma_{10})}+\phi_0, \quad (9)$$

where we use the condition that $n_0+n_1=N_0$. Thus ϕ_0 and $(\sigma_{01}+\sigma_{10})$ are determinable from measurements of n_0/N_0 as a function of the amount of gas traversed.

[11] Experimental observation supporting this assumption will be given later in this paper (Sec. IV).

III. DESCRIPTION OF EXPERIMENTAL APPARATUS AND PROCEDURES

As noted in Sec. I, this paper reports the results of several separate experiments. The heavy ion physics Cockcroft-Walton accelerator, described briefly in (I), furnished ions for the experiments over the energy range from 20 to 200 kev. Since intensity limitations precluded work at lower energies on this accelerator, a separate facility was assembled to extend the measurements to approximately 3 kev. In the Cockcroft-Walton work, the formation of negative ions was sufficiently improbable that they could be neglected. A significant number of negative ions were formed in the low-energy (3 to 30 kev) experiments, and their behavior was studied.

Different equipment and techniques were used in the separate experiments reported by this paper. Therefore, after a section of general experimental considerations, a section will be devoted to each phase of the work.

A. General

The ion source used for all of these experiments was a Phillips ionization gauge type.[12] After acceleration the proton beam was selected by magnetic analysis. The energy for both the Cockcroft-Walton and the low-energy experiments was measured and stabilized as outlined in (I). For the Cockcroft-Walton work, the error in the particle energy measurement is believed to be less than one percent. In the low-energy experiments, the distribution in energy of the ions emitted by this type of ion source (approximately 100 ev) can introduce an energy uncertainty of several percent at 3 kev.

The target gases used in these experiments were good grade compressed gases passed over cold traps maintained at liquid nitrogen temperature. In much of the work, additional purification procedures were used. Hydrogen was passed through a heated palladium barrier. Helium was passed through an active charcoal trap cooled to liquid nitrogen temperature. Neon and argon were passed over calcium and copper turnings, heated to approximately 600°C. In no case were the measured cross sections altered by the purification techniques, indicating that the feed gases were relatively pure and that the charge exchange cross sections are not sensitive to the small contamination by gases not removed by liquid nitrogen traps. This results from the fact that the cross sections are of the same order of magnitude for the noncondensable gases.

The pressures in the charge exchange chambers were monitored by a modified Alphatron gauge[13] and were measured with liquid-nitrogen-trapped McLeod gauges. Calibrations of the McLeod gauges during construction are believed to have been correct to better than one percent. Three independently calibrated gauges have been used interchangeably during the course of these

[12] Barnett, Stier, and Evans, Rev. Sci. Instr. 24, 394 (1955).

[13] National Research Corporation, Cambridge, Massachusetts.

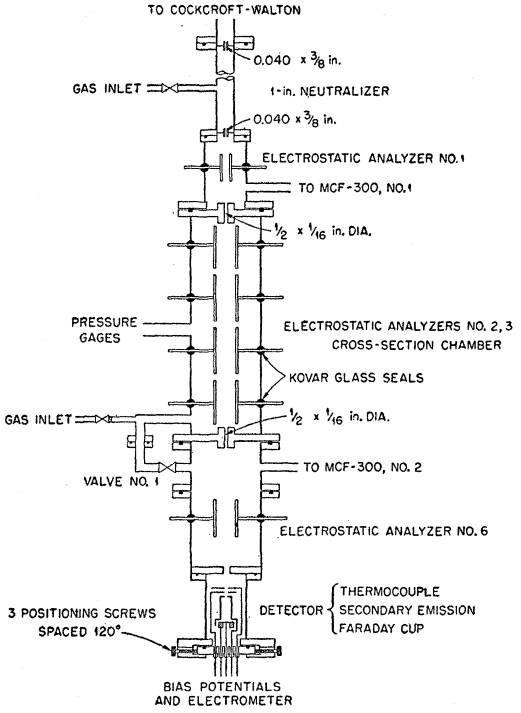

FIG. 1. Apparatus for electron loss cross-section measurement (20–200 kev).

experiments, indicating the reliability of these calibrations.

As a particle beam passes through a stopping material, the beam is broadened by multiple elastic collisions. The magnitude of this scattering is determined by the velocity of the particle and the relative masses of the incident and target atoms. It is evident that the hydrogen beam transmitted through a charge exchange chamber such as shown in Fig. 1 has been attenuated by elastic scattering. This is of no consequence provided the cross sections for elastic scattering of an ion and an atom by a target atom are the same or small compared to the inelastic cross section of interest. In the present experiments the latter condition was not always met. To ascertain whether the scattering of an ion and an atom were the same, a comparison was made of the elastic attenuation of an initially atomic beam with that of an ionic beam. Within the experimental error, no difference in elastic scattering could be detected. The test was made considerably less sensitive by the fact that both incident beams rapidly approach charge equilibrium. Hence for conveniently measured attenuations, both beams are at or near charge equilibrium over part of their range. More definitive tests for errors due to elastic scattering will be discussed in Sec. III F.

The charge exchange chamber in each of the experiments was a windowless differentially-pumped gas cell. The pumping speed and aperture sizes were chosen for approximately 100 to 1 pressure drop between the gas cell and external chamber. In each apparatus the pressure in the external vacuum system was in the range of 1 to 5×10^{-5} mm Hg. The effective path length for charge exchange will be discussed below for each experiment.

B. High-Energy (20–200 kev) Measurements of σ_{01}

A schematic diagram of the apparatus used for the measurement of the electron loss cross sections is shown schematically in Fig. 1. The first gas cell, designated the neutralizer, converted a portion of the ion beam from the accelerator to fast atoms by charge exchange. The electrostatic deflection plates (electrostatic analyzer No. 1) removed all ions emerging from the neutralizer so that the particle beam incident on the second gas cell could be entirely fast neutral atoms. Within the second chamber, ions formed by electron loss could be removed by the transverse electric field between the deflection plates. Since an ion must travel a finite distance in the electric field to be deflected enough to be removed by the collimating aperture, the effective length of the analyzing plates is slightly different from their geometric length. By segmenting the deflection plates, and applying the field to successive sections, it was possible to determine the effective length of each section experimentally. Effective lengths determined in this manner agreed well with calculated values and the presented cross sections have been computed using these effective lengths. The maximum difference between effective and geometric plate lengths was approximately 5% at 200 kev.

The detectors used were similar to the combination foil thermocouple and secondary electron emission detector described in (I). Most of the electron loss cross sections presented here were measured using secondary electron collection. Using the foil differential thermocouple as a charge insensitive detector, the relative coefficients for electron emission due to atom and ion bombardment were determined for the detector used, and were the same as those reported in (I) within the experimental error. Analyzer No. 6 in Fig. 1 was used to measure the relative number of ions and atoms in

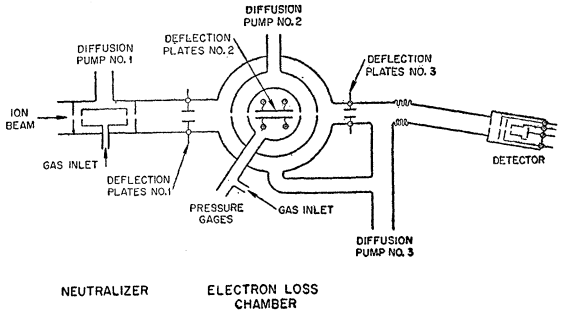

FIG. 2. Apparatus for electron loss cross-section measurement (low energy).

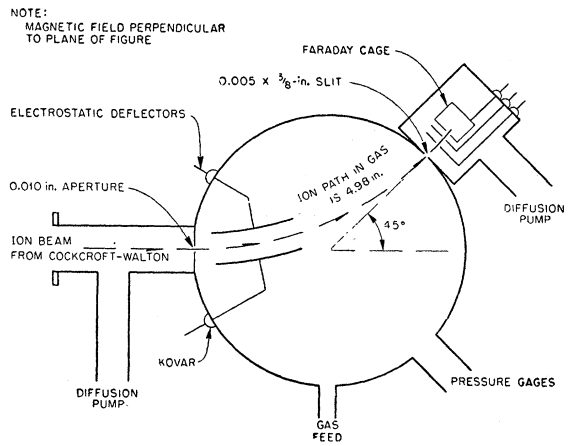

FIG. 3. Apparatus for electron capture cross-section measurement (high energy).

the particle beam emerging from the charge exchange chamber for purposes of this correction.

It is evident that the fraction of the particle beam which was neutral at equilibrium (π large) is readily measured with the apparatus. An equilibrium charge distribution could be obtained from the ion beam, either in the neutralizer or in the charge exchange chamber. It was also possible to approach charge equilibrium from an initially atomic beam. Further, in accordance with Eq. (9), the sum of the cross section $(\sigma_{01}+\sigma_{10})$ could be obtained.

C. Low-Energy (3–30 kev) Measurement $(\sigma_{01}+\sigma_{0-1})$, $(\phi_{-1})/(\phi_{+1})$, and ϕ_0 [14]

The apparatus used for this phase of the work is shown schematically in Fig. 2, and is similar in many respects to that described in III B. Making use of charge exchange in the first differentially pumped gas cell, the particle beam incident on the second gas cell could be entirely atomic or have an equilibrium distribution in charge. Application of the electric field within the gas removed ions as formed, and the cross section $(\sigma_{01}+\sigma_{0-1})$ was computed from the observed attenuation of the transmitted beam. The bellows and the third pair of electrostatic deflection plates permitted measurement of the relative intensity of the positive, negative and neutral components. The detector, described in (I), was used as a Faraday cage for ion beams and as a secondary electron emission detector for atomic or mixed beams. The intensity of the transmitted beams was too small for convenient thermocouple detection. However, it was possible to avoid the problem of the possibly differing secondary electron emission for ions and atoms by insuring that only neutrals or only equilibrium charge distributions were incident on the detector. Thus measurements of ϕ_0 were made by equilibrating the beam in the first gas cell and then passing both the total beam and the neutral component through enough gas in the second cell to re-establish equilibrium. By this procedure, the secondary electron emission was due to a particle flux with equilibrium charge distribution. Also the attenuation observed for the computation of $(\sigma_{01}+\sigma_{0-1})$ was the change in the neutral component at analyzer No. 3 caused by applying field within the charge exchange chamber. This was equivalent to recording the attenuation of a neutral beam incident on the second gas cell in view of the fact that for an equilibrium beam emergent from neutralizer, the particle flux at the detector was the same whether electrostatic deflection plates No. 1 or No. 3 were energized. Both of these procedures require that the elastic scattering of ions and atoms be approximately the same. This will be shown to be sufficiently well satisfied in Sec. III F.

The effective path length for charge exchange is taken as the entrance to exit aperture distance. In the normal procedure, when potential was applied to deflection plates No. 2 in the gas, it was also applied to deflection plate No. 3. Consequently, an ion formed near the exit aperture and not removed by plates No. 2 will be removed by plates No. 3. It is, of course, possible for such an ion to experience an electron capture collision before it reaches plates No. 3. Calculations show that under typical conditions of this experiment, only a negligible number of ions formed recapture an electron and reach the detector. Corrections for this effect have not been applied to the data since they necessitate a prohibitive number of numerical integrations.

D. High-Energy Measurement of σ_{10}

The equipment used for the Cockcroft-Walton measurements of the electron capture cross section σ_{10} is diagramed schematically in Fig. 3. The proton beam

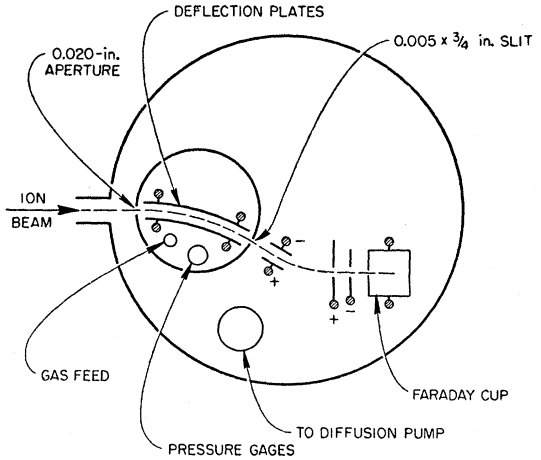

FIG. 4. Apparatus for electron capture cross-section measurement (low energy).

[14] Professor R. A. Howard of the University of Oklahoma contributed substantially to the work described in this section while a summer participant at ORNL.

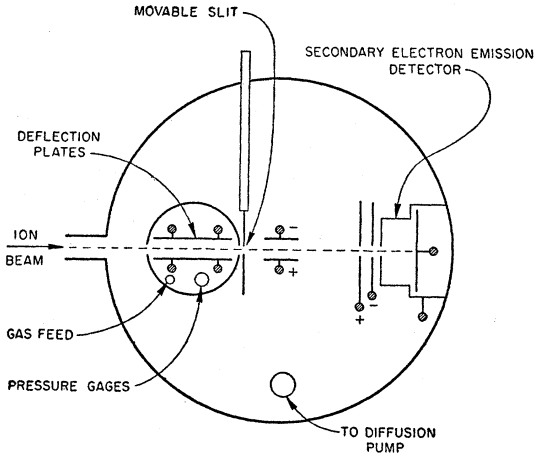

FIG. 5. Apparatus for investigation of elastic scattering effects.

after magnetic analysis entered a differentially pumped gas cell and was deflected through an angle of 45° by a transverse magnetic field. In order to avoid attenuation of the ion beam due to small-angle elastic scattering and maintain the advantages of having the detector in a high-vacuum space, the ion beam was moved across an exit slit by a linear electrostatic sweep voltage. The emergent beam was integrated. Recorder traces of the detector current as the beam was moved across the slit demonstrated the amount of elastic scattering and the number of ions which suffered two charge exchange events. For the energies and pressures used in these experiments, a negligible fraction of the ions reaching the detector had captured and lost an electron. If this were not true, the measured cross section would have been pressure-dependent and the strip-chart record of the proton current received at the detector as the electrostatic field was varied would have shown an asymmetric "tail" on the long radius of curvature side. Experimentally such a tail was observed to occur at considerably higher pressures than used for the reported cross-section measurements.

The detector was a simple Faraday cup with saturation bias voltages applied to the guard electrodes.

It is to be noted that this experiment differs from those described in III B and III C in that the charge exchange chamber was alternately at high vacuum and at a pressure of a few microns. A small change in the flux of protons which enter the chamber was caused by elastic scattering from the gas escaping through the

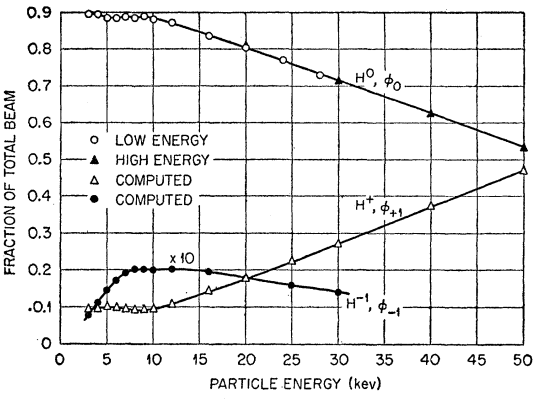

FIG. 7. Fraction of beam in +1, 0, −1 charge state after passage through "thick" target. H in hydrogen.

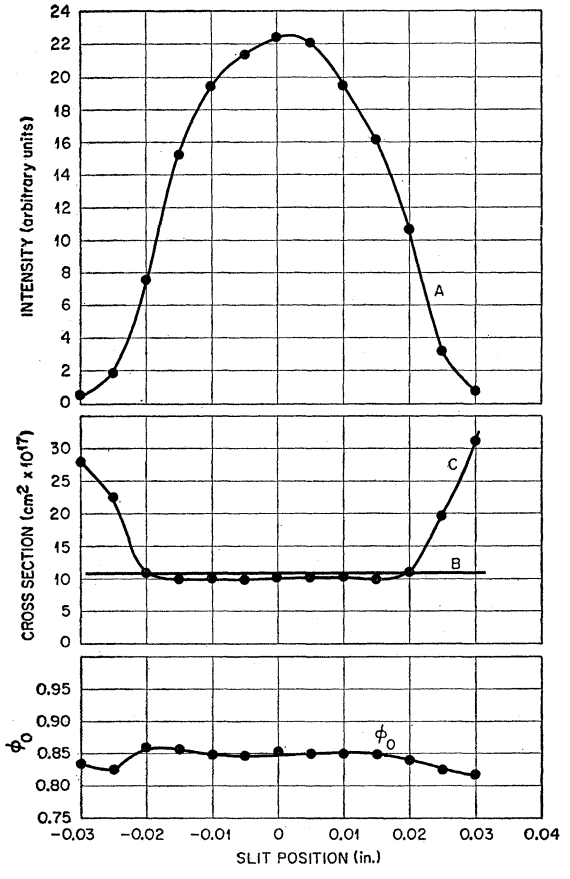

FIG. 6. The variation of intensity, cross section, and ϕ_0 with slit position. H in nitrogen at 4 kev.

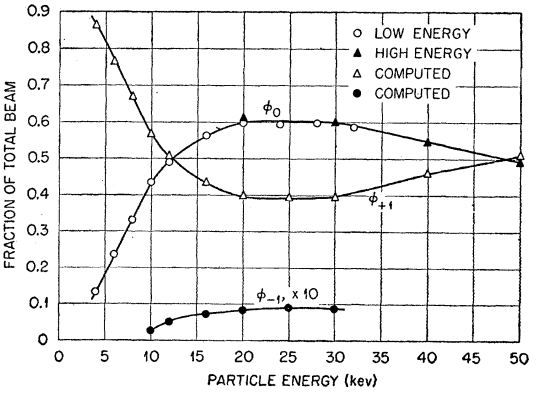

FIG. 8. Fraction of beam in +1, 0, −1 charge state after passage through "thick" target. H in helium.

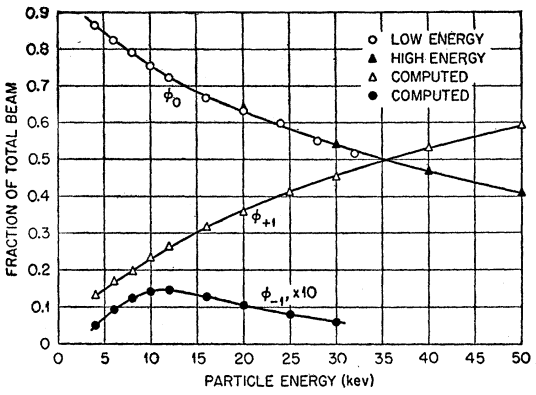

FIG. 9. Fraction of beam in +1, 0, −1 charge state after passage through "thick" target. H in nitrogen.

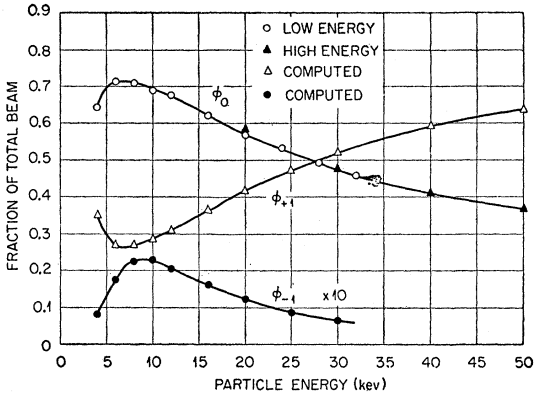

FIG. 11. Fraction of beam in +1, 0, −1 charge state after passage through "thick" target. H in neon.

entrance aperture. In order to avoid this error gas was leaked outside the entrance aperture and exit slit so that vacuum conditions in these regions were the same with and without gas in the charge exchange chamber. The differential pumping capacity was such that the pressure in these regions was from 1 to 5×10^{-5} mm Hg.

The path length was taken as the distance along the curve from the entrance to exit aperture.

E. Low-Energy Measurement of σ_{10} and σ_{-10}

The measurements of the cross sections σ_{10} and σ_{-10} in the 3 to 30 kev region were very similar to the corresponding Cockcroft-Walton work. As diagramed in Fig. 4, the proton beam was passed through a differentially pumped gas cell. The emergent beam was resolved into the −1, 0 and +1 components. The second chamber was equivalent to that described in Sec. III D, except that electrostatic deflection was used instead of magnetic deflection. A small linear sweep voltage was superimposed to move the deflected beam across the exit slit and the emergent beam was integrated as described above. In other respects the techniques discussed in Sec. III D were employed.

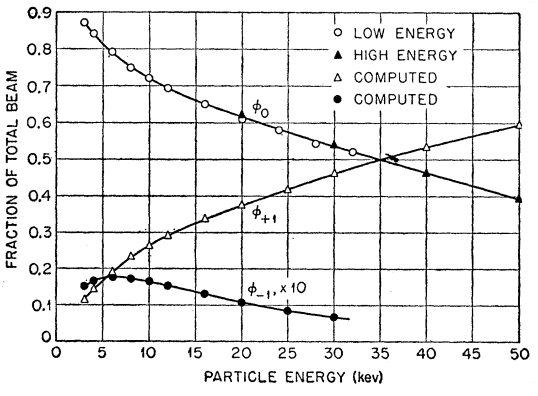

FIG. 10. Fraction of beam in +1, 0, −1 charge state after passage through "thick" target. H in oxygen.

The entrance aperture was 0.020 and 0.040 inch for the σ_{10} and σ_{-10} measurements, respectively, and the exit slit widths were 0.005 and 0.015 inch respectively. These enlarged dimensions for the negative ion work were dictated by the reduced intensities available, and were allowable in view of the lower chamber pressures needed for reliable measurements of the relatively large σ_{-10} cross sections. In all cases the differential pumping capacities were sufficient to maintain pressures of 1 to 5×10^{-5} mm Hg in the regions outside of the charge exchange chamber.

Calculations comparable to those indicated in Sec. III C show that only a very small fraction of atoms formed by charge exchange are re-ionized and reach the detector. The effective length is taken as the full path length in the gas.

F. Low-Energy Measurements of $(\sigma_{01}+\sigma_{0-1})$ and ϕ_0 by Integration[15]

As was discussed in Sec. III B, the deneutralization cross-section measurements described in Sec. III B and

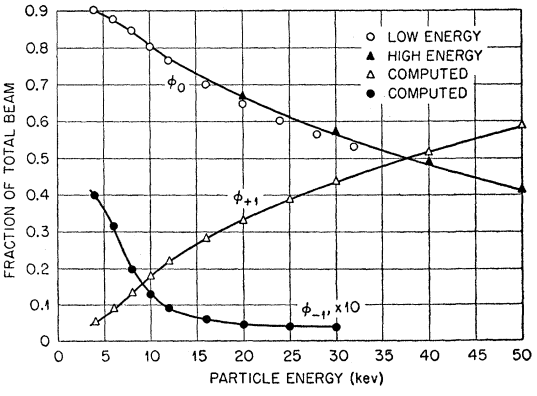

FIG. 12. Fraction of beam in +1, 0, −1 charge state after passage through "thick" target. H in argon.

[15] We wish to thank Mr. W. A. Bugg for performing much of the work described in this section while he was a summer employee at the Laboratory.

III C require that the elastic scattering cross section be the same for fast atoms and ions, or that it be small by comparison with the charge exchange cross sections. This section describes further experiments designed to test this condition.

Upon completion of the measurements described in Sec. III E, the apparatus was modified as depicted in Fig. 5. Deflection plates were installed to establish an electrostatic field perpendicular to the beam axis, and a movable exit slit was installed. The slit was moved at a constant linear rate across the beam axis by a motor driven shaft through the vacuum wall. The current through the slit was integrated as discussed in Sec. III D. An additional set of deflection plates were installed between the exit slit and the secondary electron emission detector, to prevent any ions formed near the exit slit from reaching the detector.

The deneutralization cross section was calculated from the attenuation of the integrated beam (1) as voltage was applied at constant pressure or (2) as target gas was introduced for constant voltage. Both of these measurements should be insensitive to elastic scattering. Thus, if the elastic scattering cross section for ions was significantly different from that for atoms the cross sections obtained in determinations (1) and (2) would differ from the results obtained by the procedure of Sec. III C. The results of the various determinations are shown in Fig. 6. In the top half of the figure (Curve *A*), the envelope of the beam is plotted on an arbitrary intensity scale in order to orient the observed variations in cross sections. In the lower portion of the figure the values of the cross sections determined by integration in procedures (1) and (2) are shown as the horizontal line *B*. The variation of the cross section as a function of position in the beam is shown as Curve *C*. These data were taken by moving the slit across the beam by increments, and for constant pressure, observing the attenuation as voltage is applied by the procedure of Sec. III C. The cross section was independent of position near the center of the beam but rose sharply at the periphery (Curve *C*, Fig. 6). This interesting feature may be ascribed to electron loss collisions in which elastic scattering occurs. Particles which were elastically scattered to form the periphery of the beam had usually undergone charge exchange. Hence the attenuation, or apparent cross section observed as the field was applied, was larger for these regions. However, only a few percent of the beam was contained in this peripheral shell, and the cross section determined at the center of the beam was very nearly equal to the result obtained by integration. The data shown in the figure were measured at 4 kev, where the

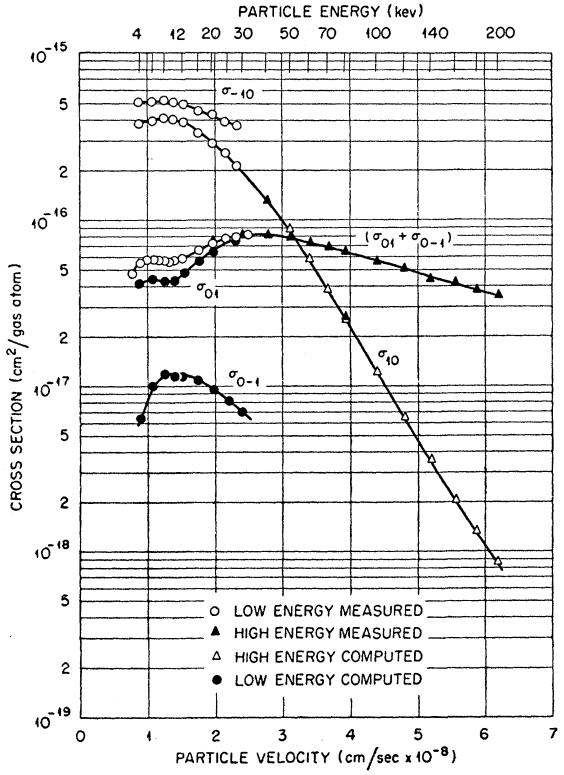

FIG. 13. The charge transfer cross sections per atom of gas traversed as a function of particle velocity or energy. Hydrogen atoms and ions in hydrogen gas.

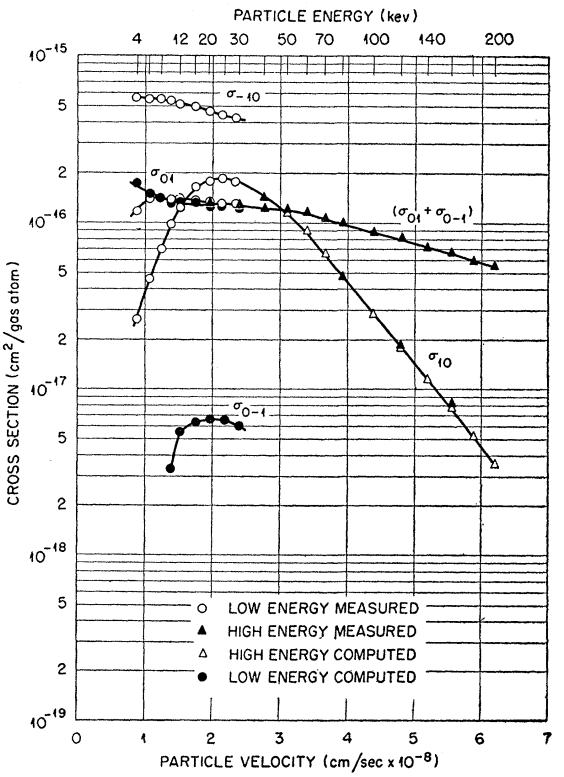

FIG. 14. The charge transfer cross sections per atom of gas traversed as a function of particle velocity or energy. Hydrogen atoms and ions in helium gas.

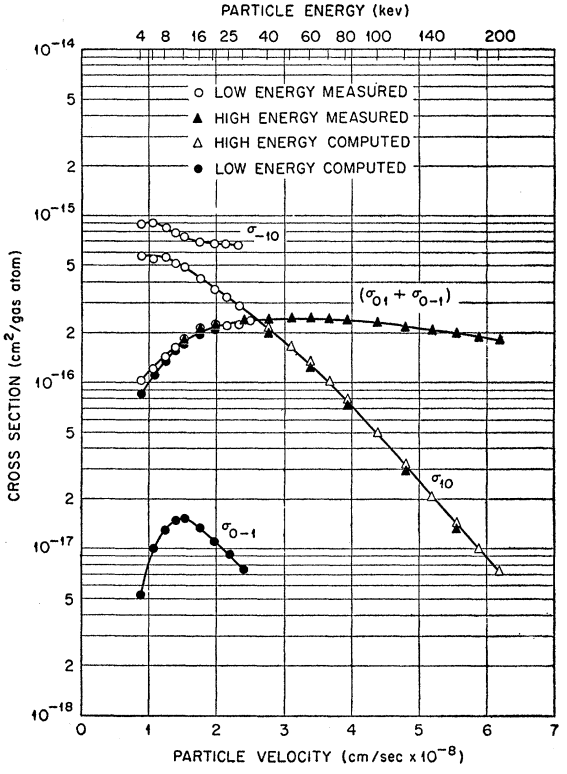

FIG. 15. The charge transfer cross sections per atom of gas traversed as a function of particle velocity and energy. Hydrogen atoms and ions in nitrogen gas.

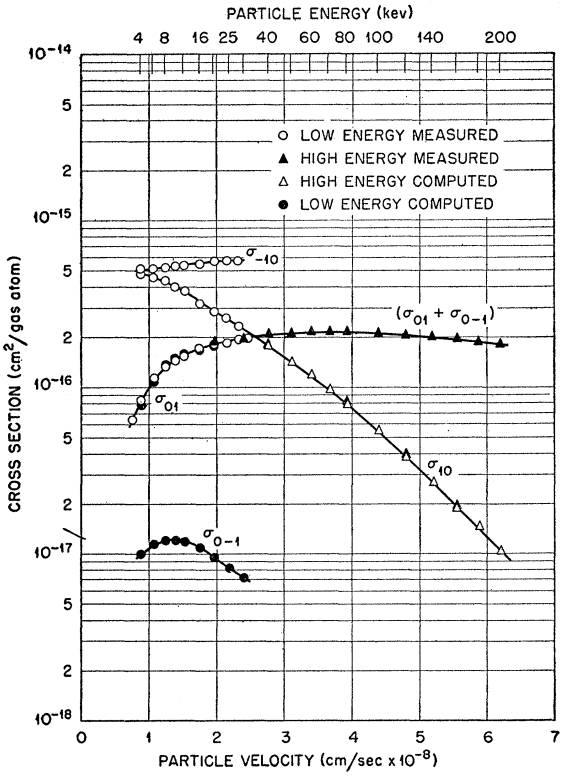

FIG. 16. The charge transfer cross sections per atom of gas traversed as a function of particle velocity and energy. Hydrogen atoms and ions in oxygen gas.

effects of elastic scattering are largest. No effect could be detected above 10 kev.

The curve ϕ_0 of Fig. 6 depicts the variation of the neutral fraction of an equilibrium beam with position in the beam. The periphery of the beam was slightly deficient in neutral atoms, as would be expected from the observed increase in cross section.

IV. RESULTS

The experimental results of this series of experiments are presented in Figs. 7 to 18. Subsequent figures show the agreement of the present results with the more recent measurements by other workers.

The variation of the equilibrium fraction of the particle beam in each of the charge states is shown as a function of energy in Figs. 7 to 12. These data were obtained by the methods described in Sec. III C. The particle beam was passed through enough gas for equilibrium to be established between competing electron capture and loss reactions. In each of the figures, the open circles of the ϕ_0 curves represent the neutral fractions measured in the low-energy experiment, while the solid triangles on these curves are data taken in the Cockcroft-Walton experiment. In all cases good agreement is obtained between the low-energy data, data measured using the Cockcroft-Walton as described in III B, and the results previously reported, (I). The ϕ_{+1} and ϕ_{-1} curves were computed from ϕ_0 and the measured ratio of negative to positive ion components, i.e., ϕ_{-1}/ϕ_{+1}, with the requirement that $(\phi_{-1}+\phi_0+\phi_{+1})=1$. Attention is called to the fact that the ordinate for ϕ_{-1} is expanded by a factor of ten in each of these figures for clarity in presentation. Referring to the figures, it will be seen that at 40 kev, one percent or less of the hydrogen beam is H^-. Therefore, it has been neglected in computations at higher energies.

The cross sections for charge transfer measured in this series of experiments are presented as functions of particle energy and velocity in Figs. 13 to 18. For the curves representing σ_{-10}, σ_{10} and $(\sigma_{01}+\sigma_{0-1})$ the points are the average of the several measurements made at each energy, and the small scatter, rarely more than one percent, of the data around the smooth curves indicate the relative accuracy of the measurements. The open circles represent the results of the low-energy measurements (Sec. III C and E), while the triangle points represent the high-energy data (Sec. III B and D). The solid circles indicate values of the cross sections σ_{0-1} and σ_{01} computed from σ_{-10} and σ_{10} respectively, making use of the independently determined values of ϕ_{-1}/ϕ_0 and ϕ_{+1}/ϕ_0. The points designated as open triangles on the σ_{10} curve were computed from $(\sigma_{01}+\sigma_{0-1})$, which is taken to be σ_{01} for energies in excess of 40 kev (see below). Excellent agreement is

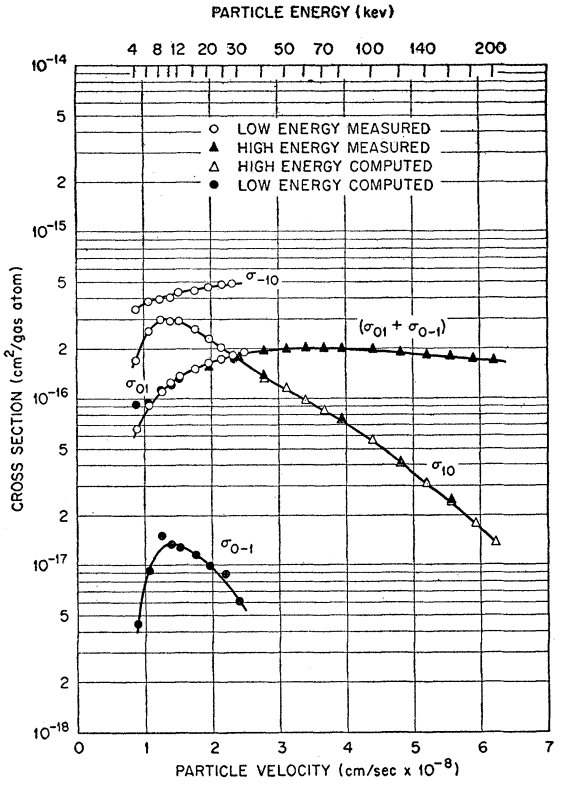

FIG. 17. The charge transfer cross sections per atom of gas traversed as a function of particle velocity and energy. Hydrogen atoms and ions in neon gas.

obtained between the separate low-energy and high-energy experiments, as evident from the smooth joining of the curves between 20 and 30 kev. Internal consistency of the series of experiments is tested by the agreement of the sum of the computed σ_{0-1} and σ_{01} curves and the experimental $(\sigma_{01}+\sigma_{0-1})$ curve. Reference to the figures shows that the agreement is within the cumulative experimental errors. Explicitly, the computed deneutralization cross section is given in terms of the experimental measurables σ_{10}, σ_{-10}, ϕ_0, and ϕ_{-1}/ϕ_{+1} as

$$\sigma_{01}+\sigma_{0-1}=\sigma_{10}\left[\frac{(1/\phi_0)-1}{1+(\phi_{-1}/\phi_{+1})}\right]+\sigma_{-10}\left[\frac{(1/\phi_0)-1}{1+(\phi_{+1}/\phi_{-1})}\right].$$

V. ERRORS

As stated in the previous section, the relative accuracy and internal consistency of the data obtained in this series of experiments is best demonstrated by the small scatter of the individual determinations about the smooth curves and by the smooth joining of the results of the low- and high-energy experiments. Also good agreement is obtained between the measured deneutralization cross section $(\sigma_{01}+\sigma_{0-1})$ and this cross section computed from the other measurables σ_{10}, σ_{-10}, ϕ_0 and ϕ_{-1}/ϕ_{+1}. Such observations indicate that the relative errors are less than 5% for all reported data. It is believed that the error in the absolute values of the measured cross sections does not exceed 5% except for incident energies less than 10 kev where the error may be as large as 10%. The various instrumental errors have been discussed in the sections devoted to the description of the apparatus. Estimates were given in these sections of the precision of measurement of the particle energy, the effective length of the exchange gas, the pressure of this gas, and of the effects of its purity. The above estimates of probable errors were obtained by consideration of the errors in the separate experiments and of the internal consistency of the results. The larger error ascribed to the very low-energy work reflects the larger energy uncertainty and the increased importance of elastic scattering.

VI. DISCUSSION

The two types of behavior of the charge composition after passage through an infinitely thick target are exemplified by the curves in helium and argon (Figs. 8 and 12). At the lower energies in argon, hydrogen, nitrogen, and oxygen, most of the fast hydrogens are neutral. By comparison, in helium at corresponding energies, most of the beam is in the +1 charge state. These observations correspond to the fact that while

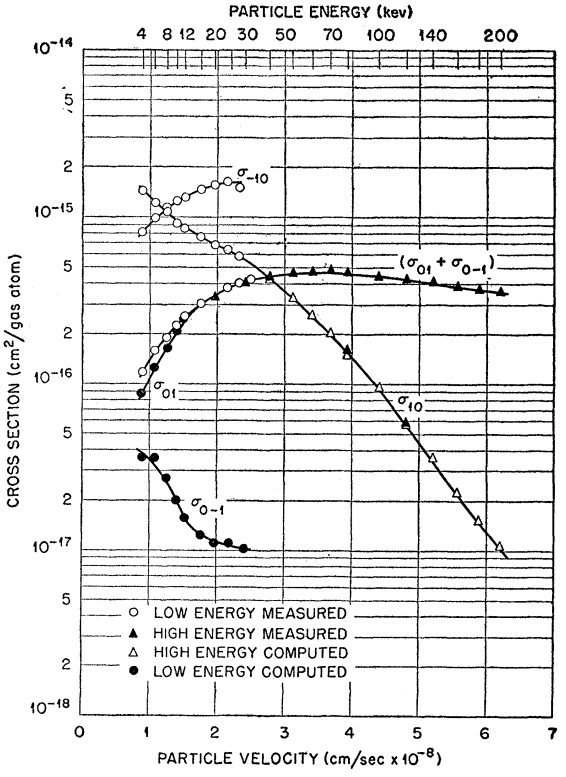

FIG. 18. The charge transfer cross sections per atom of gas traversed as a function of particle velocity and energy. Hydrogen atoms and ions in argon gas.

passing through an easily ionized gas, e.g., argon, protons readily capture electrons. On the other hand, a proton has difficulty removing an electron from the tightly bound helium atom, although a fast hydrogen atom may be ionized in a collision with a helium atom. The behavior in neon is intermediate between helium and argon. It is only at the lowest energies studied, i.e., nearest to the adiabatic condition, that the proton is ineffective in removing an electron from the neon atom. It should be pointed out that this behavior is equivalent to that reported in (I) for argon ions in helium and neon at considerably higher energies. These qualitative statements will be discussed in terms of the separate cross sections below.

Attention is called to the unique behavior of the ϕ_0 and ϕ_1 curves in hydrogen gas in the energy region 3 to 10 kev. Throughout this energy range, the neutral component is approximately constant, and in fact, shows a slight local minimum. As will be shown below, this results from a subsidiary maximum in the cross section for electron loss, σ_{01}.

It is to be noted from the sequence of Figs. 13 to 18 that the velocity behavior of the σ_{-10} cross section resembles that of the σ_{01}, while the σ_{10} and σ_{0-1} curves have similar shapes. This correspondence might be predicted, since σ_{10} and σ_{0-1} characterize electron attachment reactions, while σ_{-10} and σ_{01} gauge electron loss processes.

In each of the gases studied, the cross section σ_{10} decreases at the higher energies very nearly as Ae^{-bv}, where A and b are constants for each gas. This behavior is most noticeable in hydrogen and helium. In the energy range studied σ_{10} decreases by about three orders of magnitude in hydrogen gas, while the observed decrease in oxygen and neon was only about a factor of 50.

In contrast to the rapid variation of σ_{10}, the electron loss cross section σ_{01} changes only by a factor of from 2 to 4 within this energy region. The most interesting feature of these σ_{01} curves is the subsidiary maximum in the data for hydrogen gas. Although no detailed treatment of this feature can be given at the present, the structure is similar to that expected theoretically when double transition collisions may occur. Bates and Griffing[8] have discussed the cross sections expected for collisions between two hydrogen atoms in which both atoms may undergo electron excitations. They find that at low energies ($\sim$10 kev) single-transition collisions predominate, but at higher energies, double-transition collisions are more important. Thus the total cross section *vs* energy curves may show two maxima. In the present case, the reaction studied is an atom-atom collision in which the fast atom is ionized. The shape of the cross-section curve suggests two modes for the reaction: At low energies the stationary molecule is left in the ground state, whereas at higher energies it is likely that the stationary molecule will be left in excited or ionized states. Similar behavior might be expected for other target gases. That double maxima are not observed must be attributed to overlapping of the single and double transition cross section contributions producing a single broad maximum.

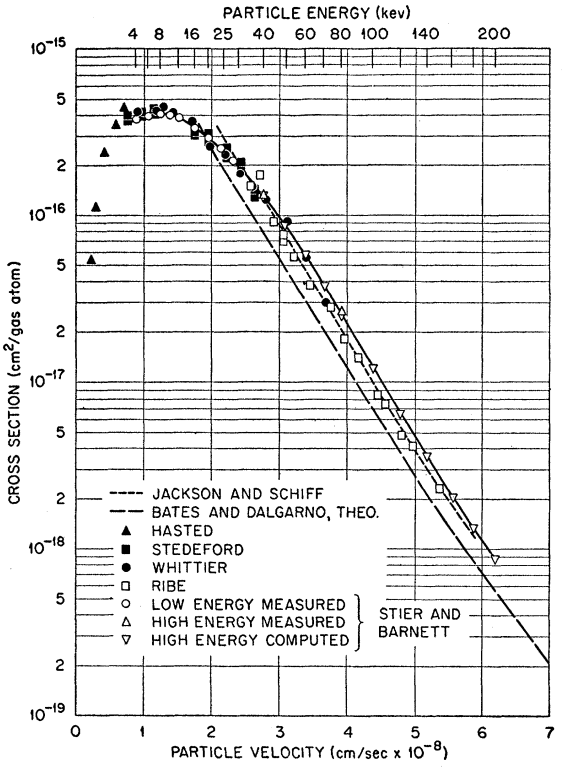

FIG. 19. σ_{10}, electron capture cross sections per atom of gas traversed. Protons in hydrogen gas.

Figure 19 is a comparison of the present electron capture cross section, σ_{10}, in hydrogen gas with recent experimental and theoretical values by other workers. The solid curve is drawn through the present data. The results of Whittier[4] and Ribe[16] were plotted from their tabulation, and the data points for Stedeford and Hasted[5] were taken from their published curve. In view of the difficulty of the experiment and the diversity of techniques used by the various investigators, the agreement may be considered excellent. The similarity between the velocity dependence of the experimental cross section and the theoretical dependence obtained by Bates and Dalgarno, and by Jackson and Schiff is also satisfying.†

A similar comparison of the data for σ_{10} in helium is given in Fig. 20. Again the solid curve has been drawn through the present data. Very striking agreement is

[16] F. L. Ribe, Phys. Rev. **83**, 1217 (1951).

† *Note added in proof.*—Dr. Bates has kindly pointed out that the curve in Fig. 19 due to Bates and Dalgarno represents their computed cross sections for capture into the ground state only. If the contributions due to excited states are included [D. R. Bates and A. Dalgarno, Proc. Phys. Soc. (London) **A66**, 972 (1953)] the agreement between the experimental and theoretical results is considerably improved.

again noted between this curve and the results of Hasted and Stedeford.[5] The theoretical curve of Bransden, Dalgarno, and King[8] shows an essentially identical dependence of the cross section on the velocity. As Griffing has pointed out,[17] the theoretical formulation is best tested by the velocity dependence of the cross section although the amplitude may be in error by a small factor due to the contributions from capture into excited states.

In Fig. 21, the present values of σ_{10} for protons in neon and argon are seen to be in excellent agreement with those of Stedeford and Hasted. The capture cross section was found to vary slightly more rapidly with velocity in oxygen than in nitrogen, as shown in Fig. 22. In this figure, the results of Kanner who measured σ_{10} in air are given for comparison.

Very few data are available in the literature for comparison with the cross sections σ_{01} or σ_{0-1} obtained in these experiments. Montague[18] and Kanner[19] have measured σ_{01} in hydrogen and in air, respectively. These experimenters obtained cross sections which are approximately 10% smaller than the values presented here. A few other results are to be found[2] but no exhaustive comparison will be made.

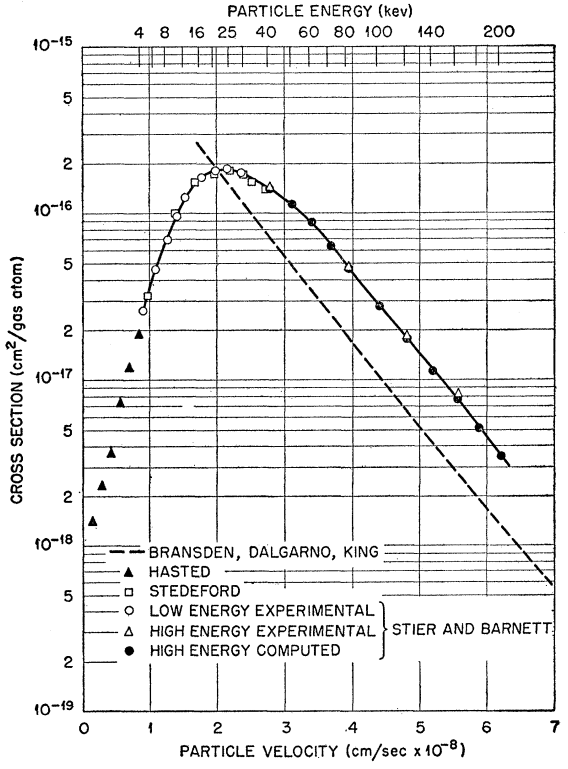

FIG. 20. σ_{10}, electron capture cross section per gas atom traversed. Protons in helium.

[17] G. Griffing (private communication).
[18] J. H. Montague, Phys. Rev. 81, 1026 (1951).
[19] H. Kanner, Phys. Rev. 84, 1211 (1951).

Stedeford and Hasted[5] have reported measurements of the detachment cross sections in the noble gases, and Whittier[4] has made similar measurements in hydrogen. Comparison of these data with the present work is made in Fig. 23 for H^- in hydrogen and helium. Each of the σ_{-10} determinations were made much less precise than the corresponding σ_{10} measurement by the very small intensity of the H^- ion beam available. In view of this the relatively poor agreement may be considered satisfactory.

It should be pointed out again that these results have been treated as though in a single collision only one electron may be transferred. No quantitative determination of the two electron transfer cross sections has been possible. It seems likely that these cross sections must be considerably smaller than the single electron transfer cross sections. This conclusion has been reached for the following experimental reasons: (1) In this rather extensive experimental program, no indication was ever present that double transitions were taking place. (2) The consistency of the results, interpreted in terms of single transitions would indicate relatively few double transitions. (3) The present measurements of σ_{10} are in such excellent agreement with those of Stedeford and Hasted, in spite of the fact that the

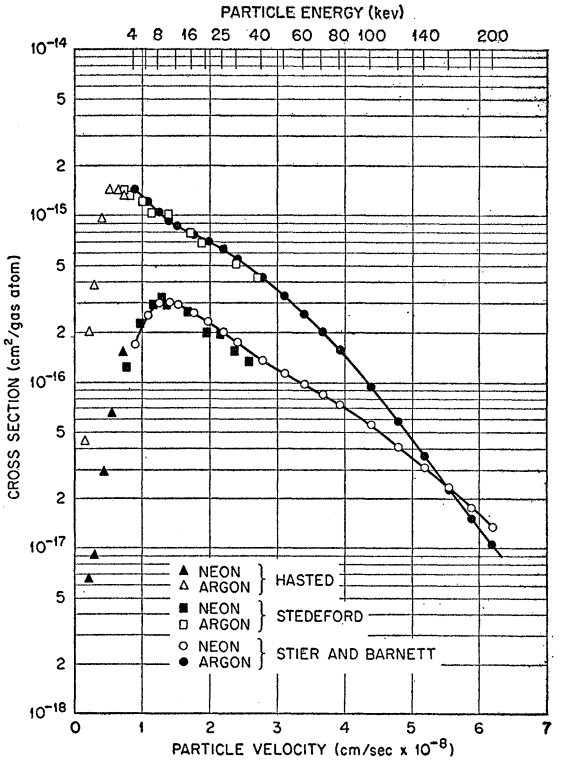

FIG. 21. σ_{10}, electron capture cross section per atom of gas traversed. Protons in neon and argon.

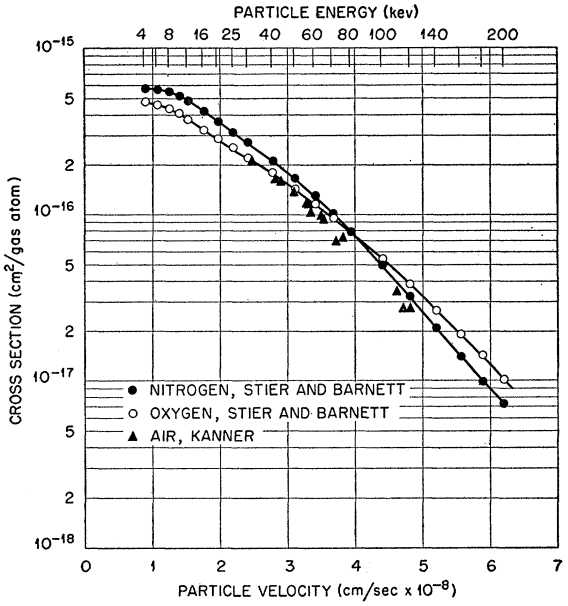

FIG. 22. σ_{10}, electron capture cross section per atom of gas traversed. Comparison of present results for protons in nitrogen and oxygen with those of Kanner in air.

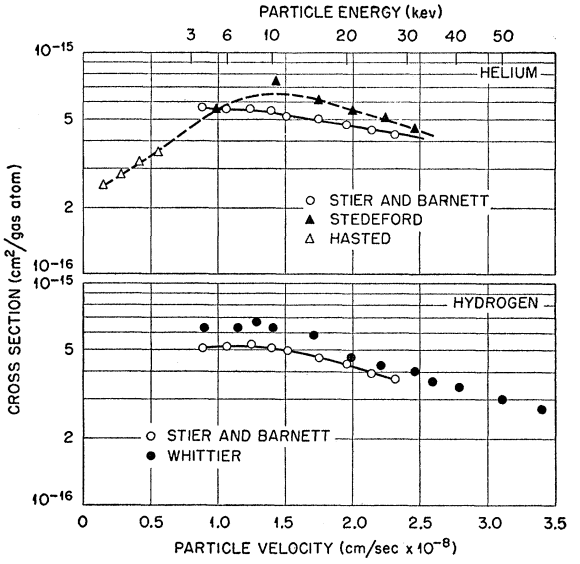

FIG. 23. σ_{-10}, electron detachment cross section per atom of gas traversed for H^- ions in hydrogen and helium.

experiment described in Sec. III D measures $(\sigma_{10}+\sigma_{1-1})$ while the Stedeford and Hasted[5] method measures $(\sigma_{10}+2\sigma_{1-1})$. In the present work the cross section was computed from the attenuation of a transmitted beam due to all charge-changing collisions. In the Stedeford and Hasted experiment, the number of slow ions formed in the target gas was measured per incident ion, and the cross section was computed from this slow ion current and the pressure according to the relation $\sigma=(I'/I)(1/nl)$ where I' is the slow ion current, I the incident current, n the gas density in atoms per cm³, and l the path length in cm. If two-electron-transfer collisions occur, e.g., $H^++A^0\rightarrow H^-+A^{++}$, the doubly charged slow ion will be "counted twice," and the equation should be rewritten in terms of the particle fluxes j as

$$\sigma_{10}+\sigma_{1-1}=\left(\frac{j_1}{j_0}+\frac{j_2}{j_0}\right)\frac{1}{nl},$$

where j_1 is the flux of singly charged slow ions, j_2 the flux of doubly charged ions and j_0 the incident flux. In this notation, their recorded currents are $I=ej_0$ and $I'=e(j_1+2j_2)$. Thus, the cross section given by Stedeford and Hasted is $\sigma_{10}+2\sigma_{1-1}$. In view of the excellent agreement between the results of these authors and the present work, one must conclude that σ_{1-} is small compared to σ_{10}.

ACKNOWLEDGMENTS

The authors wish to acknowledge helpful discussions with Dr. A. H. Snell of the Oak Ridge National Laboratory and with Professor S. K. Allison of the University of Chicago.